FEBS 20307
FEBS Letters 429 (1998) 21–26

Structural and dynamic helix geometry alterations induced by mismatch base pairs in double-helical RNA

Martin Vogtherr, Harald Schübel, Stefan Limmer*

Laboratorium für Biochemie, Universität Bayreuth, D-95440 Bayreuth, Germany

Received 18 March 1998

Abstract **A ribooligonucleotide microhelix derived from the acceptor stem of *Escherichia coli* tRNA$^{\text{Ala}}$ having a C3-A70 mismatch in place of the G3-U70 wobble pair in the wild-type tRNA$^{\text{Ala}}$, and a sequence variant with a regular U3-A70 base pair have been investigated by NMR. In vivo, suppressor tRNA$^{\text{Ala}}$ variants with C3-A70 (as well as several other) mismatch pairs are substrates for alanyl-tRNA synthetase (ARS), supporting the hypothesis of an 'indirect' recognition of the identity element 3-70 mismatch pair via structural modifications caused by the mispair in comparison to canonical A-RNA helices. It is demonstrated that the C-A mismatch likewise induces helix geometry alterations, in particular with respect to base stacking in the vicinity of the mismatch. However, with reference to the 'wild-type' G3-U70 microhelix, destacking in the C3-A70 acceptor stem duplex occurs in the opposite direction from the mismatch pair. Therefore it is concluded that the locally enhanced conformational flexibility or dynamics associated with the structural changes induced by the mismatch pairs could be an essential prerequisite for optimal adaptation of the tRNA$^{\text{Ala}}$ acceptor stem to the contact region of the ARS.**

Key words: NMR; RNA; Mismatch pair; Aminoacyl-tRNA synthetase; Helix geometry

1. Introduction

In protein biosynthesis, specifically aminoacylated tRNAs transport amino acids to the ribosomes. The correct aminoacylation of a given tRNA with its cognate amino acid is accomplished by the aminoacyl-tRNA synthetases which have to discriminate between the different tRNAs being similar with respect to secondary (Fig. 1) and tertiary structure. Specific recognition of the 'correct' tRNA, and rejection of 'wrong' tRNAs is enabled by the occurrence of recognition or 'identity' elements. These can be located in different parts of the tRNA (for reviews see [1,2]) and frequently comprise single nucleotides or base pairs. Often, they are formed by the anticodon nucleotides, or are located in the acceptor stem. One well-studied example of the latter type is represented by the G3-U70 base pair of the tRNA$^{\text{Ala}}$ from *E. coli* and eukaryotes. It has been demonstrated [3,4] to form the major identity element for the recognition by the cognate alanyl-tRNA synthetase (ARS). Even truncated tRNA molecules with only seven base pairs are suitable substrates for recognition and correct aminoacylation by the ARS [5].

The observation that replacement of the critical G3-U70 wobble pair by regular Watson-Crick pairs as well as by an I3-U70 pair (I-inosine) yields a total loss of the substrate properties [6,7] led to the conclusion that the 2-amino group of G3 is indispensable for the correct recognition by the enzyme. Other than in G-C Watson-Crick pairing, this amino group is not directly involved in hydrogen bonding and protrudes into the minor groove, thus representing a candidate for making specific contacts with the protein.

However, it has been shown that suppressor tRNA$^{\text{Ala}}$ variants are in vivo alanylated if they contain at the position 3-70 other mismatches than G-U, like G-A, C-A, or U-U [4,8,9]. These findings were corroborated by in vivo experiments with mutants of suppressor tRNA$^{\text{Lys}}$ whose identity could be switched to tRNA$^{\text{Ala}}$ by mutating the original G3-C70 pair to G3-U70 [10]. From these experiments it was concluded that direct recognition of a functional group (2-NH$_2$ of G3) alone cannot explain the recognition of the G-U wobble pair by the ARS, since not all of the 'active' suppressor tRNA mutants are equipped with mismatches which would display an amino group with a geometry in the way provided by the G-U pair. Rather, local distortions of the helix induced by the mismatches should be recognized by the ARS. Indeed, NMR studies of RNA helices derived from the tRNA$^{\text{Ala}}$ acceptor stem [11,12] suggest conformational peculiarities of the helix with a G3-U70 pair as compared to stems with canonical G3-C70 Watson-Crick pairs. In particular, a destacking between nucleotides U70 and C71 was observed that could also give rise to a locally enhanced intramolecular dynamics and flexibility.

By comparison of two acceptor stems with mismatch pairs

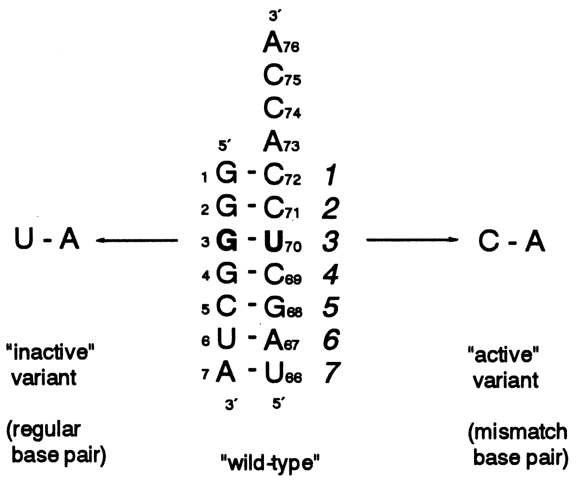

Fig. 1. Secondary structures of RNA oligonucleotides under investigation in the present study. The wild-type acceptor stem helix is shown in the middle, with the critical 3-70 base pair depicted in boldface. The two base pairs are displayed as well.

---

*Corresponding author. Fax: +49 (921) 55-2432.
E-mail: btc996@btc9x1.che.uni-bayreuth.de

PII S0014-5793(98)00542-0

(G3-U70 and C3-A70), whose suppressor tRNA^{Ala} counterparts are active substrates for the ARS [4,8,9], with acceptor stems containing Watson-Crick pairs at position 3-70 (A3-U70 and U3-A70), being no substrates for the ARS, additional insight into the effect of mismatch pairs upon local helix geometry was expected. It should be checked if the results can serve to further substantiate the concept of 'indirect recognition' of the tRNA^{Ala} by its synthetase via local helix irregularities.

2. Materials and methods

2.1. Preparation of samples

RNA oligonucleotides were chemically synthesized on a Gene Assembler Plus (Pharmacia LKB) by the H-phosphonate method [13]. The deprotected ribooligonucleotides were purified by HPLC on a DEAE 500-7 anion exchange column (Macherey-Nagel). Purification was carried out under denaturing conditions (7 M urea, 20 mM potassium phosphate buffer pH 6.3, 60°C). The RNA was separated by KCl gradients (0–1 M KCl) and subsequently desalted on a Biorad P6 column. Sample purity was checked by denaturing (7 M urea) PAGE. Concentrations were determined by UV absorption [14].

NMR samples were prepared with final RNA concentrations of ca. 1 mM and were dissolved in D_2O solution containing 100 mM NaCl, 10 mM sodium phosphate buffer. The pH was adjusted with a glass electrode (Mettler-Toledo). RNA was annealed by heating of the samples to 80°C for 3 min and subsequent slow cooling to room temperature. 2,2-Dimethyl-2-silapentane-5-sulfonate (DSS) was added as internal reference.

2.2. NMR spectroscopy

NMR spectra were recorded on a Bruker DRX 500 spectrometer at 500 mHz proton resonance frequency. In all cases, the HDO signal was suppressed by presaturation.

NOESY, TOCSY and DQF-COSY spectra were recorded phase-sensitive in t_1, with $4K$ data points in t_2, 512 t_1-increments and sweep widths of 10 ppm in both dimensions using standard pulse sequences. FIDs were apodized by $\pi/2$ shifted squared sinebell functions. NOESY spectra were recorded with mixing times of 80, 150, and 350 ms.

Heteronuclear chemical shift correlations were measured as HMQC spectra with GARP decoupling in t_2. $2K \times 512$ data points in t_2 and t_1, respectively, were measured for a carbon spectral width of 130 ppm. Carbon chemical shifts were referenced to the folded DSS ^{13}C chemical shift.

Phosphorus NMR spectra were recorded with proton decoupling. ^{31}P chemical shifts were referenced to external 85% phosphorous acid.

2.3. Data analysis

The NDEE program package (Software Symbiose, Bayreuth) was used for data analysis and assignment. The standard assignment scheme for unlabelled RNA [15] was employed for the assignment of proton resonances. From the 150 ms NOESY spectrum of the C3-A70 duplex, 127 non-trivial NOEs were extracted for structure calculation. For the G-U microhelix [11], 103 NOEs were obtained in a similar way. Homonuclear coupling constants were obtained from the DQF-COSY spectra.

Analysis of the protonation state of adenosines was achieved by heteronuclear chemical shift correlation in conjunction with the known proton chemical shifts [16,17]. The pK_a values were determined from the pH dependence of the C2 and C8 chemical shifts [17].

2.4. Structure calculation and analysis

Structure calculations were performed with the XPLOR program package [18]. A force field optimized for nucleic acids was used throughout [19], with all parameters involving hydrogen atoms being adopted from the CHARMM force field.

Structure calculations started from a random structure. A simulated annealing protocol originally proposed by Wimberly [20] was used. NOEs (cf. Section 2.3) and dihedral restraints were used. The conformation around the phosphate group was assumed to be regular due to absence of unusually shifted ^{31}P resonances [21]. The ribose was assumed to be either in pure 2′-*endo* or 3′-*endo* puckering.

Only the structures with the lowest energies were considered for further use. These were subjected to an analysis regarding dihedral angles and global helical geometry with the CURVES program [22].

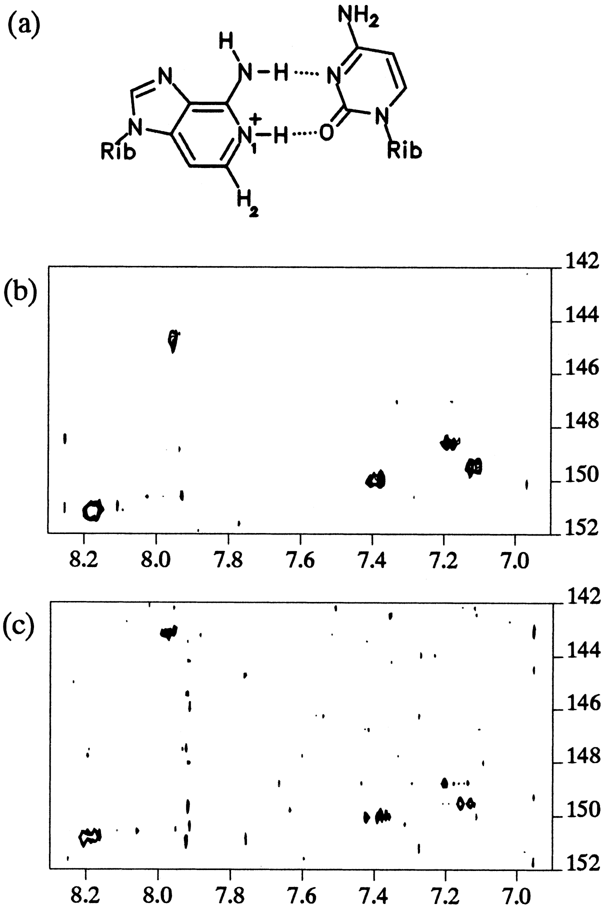

Fig. 2. a: Base-pairing scheme for CA mismatches as proposed on the basis of crystal structure analyses and NMR data in both DNA and RNA. The stability of this arrangement is increased by protonation of the adenine N1, which leads to formation of a second hydrogen bond. b and c: Region of C2-H2 correlations in the HMQC spectrum at pH 6.5 (b) and pH 5.0 (c). Whereas most adenosine C2s resonate around 150 ppm, the A70 C2 displays a pH-dependent upfield shift. A similar but much smaller effect is observed for A70 C8 which is shifted downfield.

3. Results

3.1. Geometry of the C3-A70 mismatch pair

For the arrangement of a C-A mispair different geometries are conceivable [23]. For C-A pairs in regular double-helical context, a base pair formation as depicted in Fig. 2a has been suggested on the basis of crystallographic [24,25] and NMR studies [26,27]. There, hydrogen bonds are not only formed between the C6 amino group of A and the N3 of C, but also between the protonated N1 of A$^+$H and the O2 of C. This base pair pattern was also found for C-A mismatches in helical regions of the 'leadzyme' [16,17] and the 'hairpin' ribozyme [28]. Formation of an additional hydrogen bond leads to pK_a values between 6.3 and 6.8 in contrast to a value of 3.52 for free adenosine [29]. For structural analyses knowledge of the C-A base pair geometry is indispensable. Information about the adenosine-N1 protonation can serve to characterize

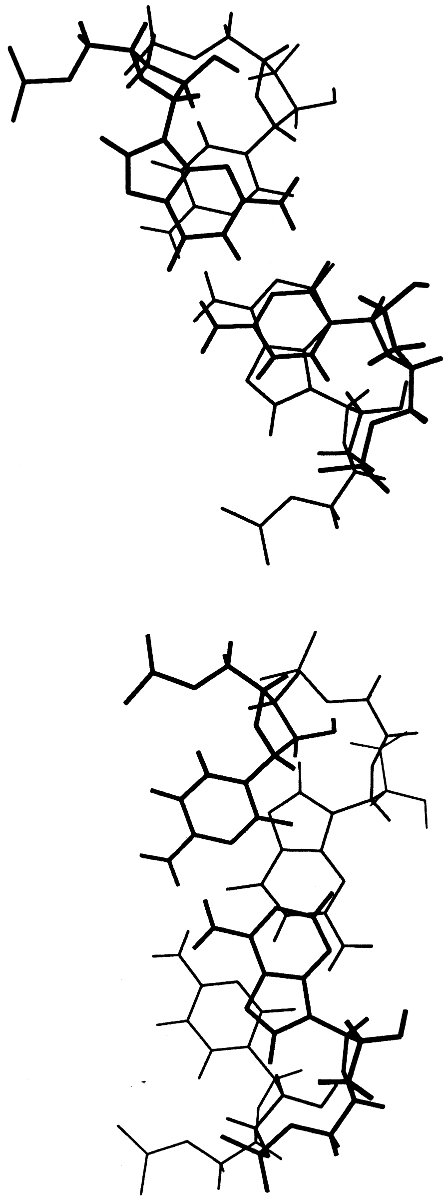

Fig. 3. Stacking interactions around the C3-A70 mismatch base pair. Top: Stacking between G2-C71 (bold) and C3-A70 base pairs; bottom: stacking between the C3-A70 (bold) and G4-C69 base pairs. The mismatch pair is well stacked above the G2-C71 pair, but destacked in the other direction with respect to the G4-C69 pair.

the hydrogen bond pattern since a protonated A^+ hints at a base-pairing scheme as sketched in Fig. 2a.

N1 protonation leads to an upfield shift of the ^{13}C resonance of the adenosine C2 from ca. 150 ppm in non-protonated A to about 142 ppm for fully protonated A^+H [16,17,28]. Fig. 2b and c show the C2-H2 region of the ^{13}C-^{1}H-HMQC spectrum at pH 6.5 and 5.2. Whereas the chemical shifts of the C2 carbon resonances of A7, A67, A73, and A76 fall into a narrow spectral region around 150 ppm, the A70 C2 signal is shifted upfield to 144.7 ppm already at pH 6.5 (Fig. 2b). This upfield shift is increased to 143.1 ppm upon lowering the pH to 5.2 (Fig. 2c). In both cases, only one resonance is observed, indicating fast exchange on the NMR timescale between protonated and unprotonated form.

From the pH dependence of the carbon chemical shifts of A70 C2 and C8, a pK_a for the protonation of A70 N1 of 6.8 ± 0.3 can be estimated comparing well with pK_as for the adenosine N1 in C-A pairs of 6.2 in loop A of the 'hairpin' ribozyme [28], and 6.5 in the 'leadzyme' [17]. Thus at near-neutral pH the N1 is largely protonated and hence involved in hydrogen bonding according to the scheme in Fig. 2a.

3.2. Construction of an NMR-based structural model of the C3-A70 acceptor helix variant

A structural model of the acceptor helix variant with a C3-A70 base pair has been derived which is compatible with the NMR data. The main features of the overall structure are a largely A-helical stem and a high degree of stacking order in the single-stranded end, continuing essentially the helical geometry of the stem, in agreement with structural data from the G3-U70 wild-type acceptor stem [11,12]. Though the precision of the structural model obtained on the basis of the restricted NMR data set cannot be very high [30], the model allows to discuss structural features which are less strongly dependent on the precision of the structure, i.e. the number of NMR-derived restraints. One of these more 'robust' structural features is the stacking geometry between adjacent bases which is reliably reproduced in different restrained molecular dynamics calculations. Another such helical parameter – being partly associated with the base stacking – is the helical twist [31,32].

Fig. 3 shows the base stacking between the critical mismatch base pair C3-A70 and its two neighboring base pairs G2-C71 (top), and G4-C69 (bottom). Obviously, there are differences in the stacking, i.e. base plane overlap, in the two opposite directions from the C-A mispair. A very pronounced stacking of the C3-A70 base pair with the G2-C71 Watson-Crick pair is contrasted by an almost total loss of stacking between the C3-A70 and G4-C69 pairs.

This finding differs from the stacking pattern found for the wild-type acceptor helix with a G3-U70 mismatch pair [11,12] where destacking occurs mainly between U70 and C71, i.e. in the opposite direction from the mismatch pair. The low-pre-

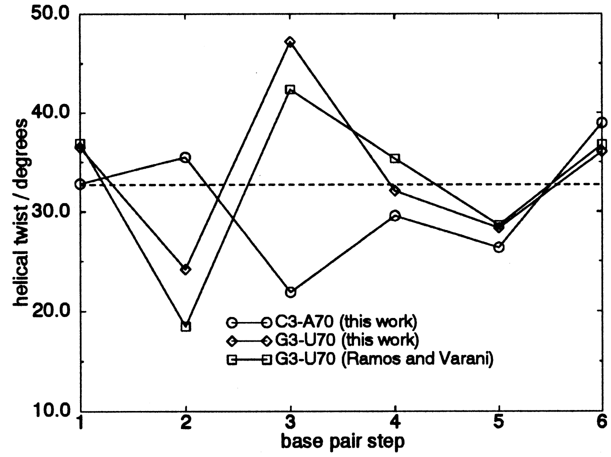

Fig. 4. Plot of the helical twist versus the base pair step for the C3-A70 mismatch duplex (circles). For comparison, the values for the wild-type acceptor stem helix (G3-U70) from a comparable NMR data set [11] (diamonds) as well as from a high-precision NMR structure [12] (squares) are plotted as well. The canonical twist angle for A-RNA (32.7°) [33] is indicated by a dashed line.

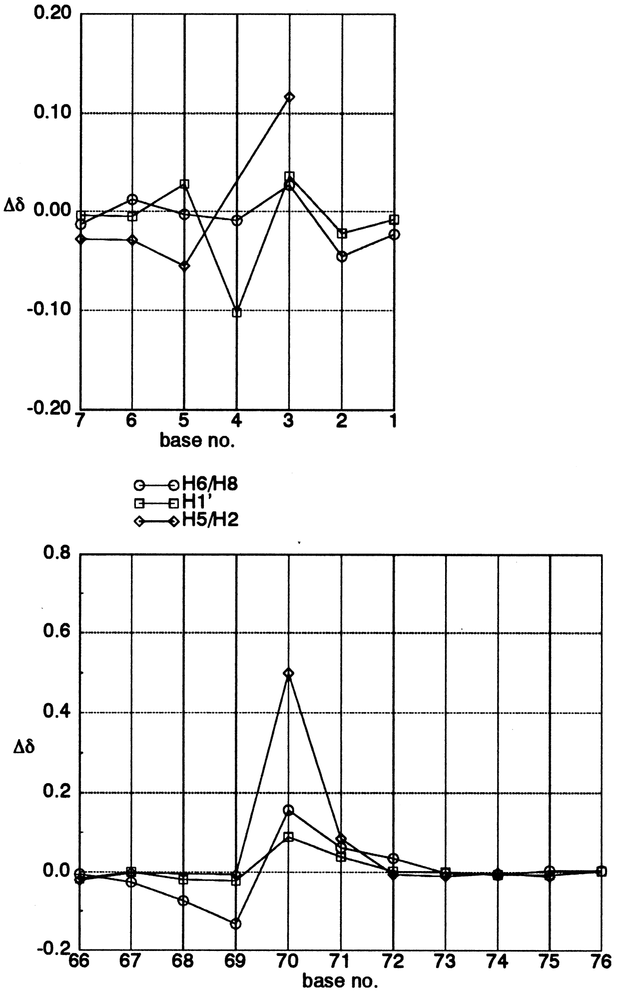

Fig. 5. Differences of chemical shifts between the acceptor stem variants with a C3-A70 mismatch pair and a U3-A70 Watson-Crick pair (cf. Fig. 1). The difference Δδ=δ(C3A70)−δ(UA70) for the aromatic (H2/H5 and H6/H8) and anomeric H1′ protons is plotted vs. the nucleotide number. The intrinsic chemical shift difference between cytosine and uracil [37] has already been accounted for.

cision structural model of the G3-U70 wild-type acceptor helix used for this evaluation was derived on the basis of a similar NMR data set as for the C3-A70 duplex (103 NOEs). A preliminary discussion of structural features of this acceptor helix has been presented already before [11].

The variant stacking geometry in the immediate neighborhood of the mismatch pairs for C3-A70 and G3-U70 acceptor stem duplexes is also reflected in the variation of helical twist along the stem which is given in Fig. 4. Whereas the helical twist between base pairs 2 (G2-C71) and 3 (G3-U70) in the wild-type acceptor helix is distinctly less (20°) than the canonical average value of ca. 32.7° [33], it is markedly increased (46°) for the steps between the third (G3-U70) and fourth (G4-C69) base pairs. These values excellently agree with those derived from the high-precision NMR structure of the wild-type acceptor helix [12], using the program CURVES [21] for the analysis of helical parameters in both the latter structure, and the one calculated on the basis of a distinctly smaller NMR data set [11]. This observation demonstrates that the helical twist does not as critically depend on the number of NMR restraints as do certain other parameters.

3.3. Comparison of the C3-A70 mismatch acceptor helix variant with a regular Watson-Crick duplex having a U3-A70 base pair: analysis of chemical shift differences

Chemical shift changes upon transition from the denatured ('coiled') state to an ordered helical duplex are brought about mainly by the ring currents of the stacked bases causing magnetic shielding effects [34–37]. Since chemical shifts, in particular those of the aromatic protons, are very sensitive to even subtle variations of the arrangement of neighboring bases, they can serve as intrinsic probes of local structural changes. This approach has been employed for characterizing the local helix geometry variations introduced by the G3-U70 wobble pair in the wild-type tRNA^{Ala} acceptor stem, as compared to a 'regular' Watson-Crick helix with a G3-C70 base pair [11]. The conclusions with respect to local stacking geometry in the vicinity of the 3-70 base pairs were confirmed by the high-precision NMR structural analysis of a closely related tRNA^{Ala} microhelix hairpin [12].

Fig. 5 shows the chemical shift differences of the aromatic and ribose 1′ protons of equivalent residues between the C3-A70 and the U3-A70 variants. It should be noted that both duplexes differ by merely one (pyrimidine) nucleotide. The intrinsic chemical shift differences between cytidine and uridine [37] have been accounted for.

As expected, significant chemical shift differences are restricted to the nucleotides C/U3 and A70, and the residues directly adjacent to the 3-70 pair. The A70H2 resonance is strongly shifted downfield in the C3-A70 duplex, as compared to the U3-A70 minihelix. This seems to correspond with a downfield shift of the U70H5 resonance in the G3-U70 wild-type duplex (in comparison to the G3-C70 variant). However, since adenosine H2 and uridine H5 occupy different positions relative to the helical axis a direct comparison would be misleading. Shift differences for the aromatic protons of C71 between C3-A70 and U3-A70 duplexes are distinctly less positive than the corresponding ones between G3-U70 and G3-C70 acceptor helices [11] though – given comparable structural variations – much larger shift changes should be expected in the former case due to the markedly stronger shielding efficiency of the adenine base [34–37]. The reverse effect is observed for the nucleotides at position 3: whereas the difference between the H6 chemical shifts is slightly positive comparing the C3-A70 and U3-A70 duplexes, the corresponding difference for the H8 shifts of G3 between G3-U70 and G3-C70 duplexes is negative [11].

This finding is paralleled by a comparison of the chemical shifts of the wild-type acceptor helix and an A3-U70 variant. Here, too, a large negative difference for the H8 chemical shifts of G3/A3 (ca. −0.27 ppm) is measured (data not shown), which is contrasted by a large positive shift difference of ca. 0.33 ppm for U70 H5 signals (i.e. a significant downfield shift of the U70H5 resonance in the G3-U70 duplex). In addition, the G4H8 resonance is upfield shifted in both the A3-U70 and G3-C70 Watson-Crick duplexes, as compared to the wild-type G3-U70 acceptor stem. By contrast, the difference between the G4H8 chemical shifts in the C3-A70/U3-A70 couple is slightly negative (Fig. 5).

Thus, at first sight, the plots of chemical shift differences between C3-A70 and U3-A70 acceptor duplex variants on the one hand, and G3-U70 (wild-type) and A3-U70 (G3-C70) acceptor microhelices on the other hand, seem to indicate similar stacking differences between 'active' (G3-U70, C3-

A70) and 'inactive' (A3-U70/G3-C70, U3-A70) variants, respectively. However, a thorough scrutiny reveals subtle, but significant deviations between the two data sets which are compatible with the alterations in the stacking-destacking pattern found between the second, third (mismatch), and fourth base pairs of the G3-U70 and C3-A70 mismatch acceptor stem duplexes, in the NOE-based structural models described before.

4. Discussion

On the basis of NMR data, the structural peculiarities in the vicinity of mismatch (G-U and C-A) base pairs within the acceptor stem helices of tRNA^{Ala} from *E. coli* have been characterized. In vivo, a suppressor tRNA^{Ala} variant containing a C3-A70 mismatch pair in place of the G3-U70 wobble pair found in wild-type tRNA^{Ala} is almost as efficiently charged with alanine as the wild-type tRNA^{Ala} [4,8–10]. However, microhelix variants comprising only the seven base pairs within the acceptor stem with a C3-A70 mispair are no substrates for the alanyl-tRNA synthetase in vitro [38], in contrast to the wild-type G3-U70 microhelix [5].

It has been shown earlier [11,12] that the specific G3-U70 pair causes modifications of the regular A-helical geometry in comparison to a duplex with a G3-C70 Watson-Crick pair. In particular, the pyrimidines U70 and C71 are destacked in the wild-type tRNA^{Ala} acceptor helix. Comparison of this wild-type microhelix with another canonical tRNA^{Ala} acceptor helix variant with a A3-U70 pair, which is likewise no substrate for the ARS, essentially corroborates these findings (data not shown). The chemical shift differences of aromatic and 1′ ribose resonances between wild-type and A3-U70 microhelices versus nucleotide number display a course which is very similar to the one found for the comparison of wild-type G3-U70 acceptor stem and a regular G3-C70 variant [11]. However, structural characterization of the C3-A70 acceptor stem helix variant reveals that in this case a pronounced destacking occurs between the mismatch pair bases, and the bases of the fourth pair (G4-C69) (Fig. 4). For the pyrimidine base (C3), the loss of base plane overlap, compared to a regular Watson-Crick helix, seems to be still more dramatic than for the base paired purine (A70).

Apparently, destacking is – as in the case of the wild-type G3-U70 acceptor stem – achieved by swivelling the pyrimidine of the mismatch towards the major groove, and the purine into the minor groove. In case of the C3-A70 variant, the axis of rotation seems to be almost in the center of the base pair, whereas for the G3-U70 wild-type acceptor stem this local rotation axis for the mispair swivelling motion should be shifted towards the G3, giving rise to an apparently stronger displacement of the uridine-70. Obviously, destacking occurs in opposite directions from the mismatch base pairs in G3-U70 and C3-A70 acceptor stem variants, respectively, in comparison to the regular duplexes (G3-C70/A3-U70, and U3-A70, respectively).

These findings might imply that for recognition of the corresponding tRNA^{Ala} variants by the ARS not a specific type of irregularity, e.g. a certain local or position-specific destacking of bases near the mismatch pair, is important but rather the altered helical geometry in general. Destacking of nucleotide bases gives rise to decreased stacking interactions between adjacent bases which represent the most important stabilizing interactions in double-helical nucleic acids. Introduction of G-U, G-A, C-A, U-U, and other mismatch pairs consequently diminishes the overall thermodynamic stability in double-helical oligonucleotides [39–42]. Hence, such mismatch pairs not only give rise to (static) distortions of regular A-helical geometry, but also to a locally enhanced structural flexibility. This flexibility might, in its turn, be required to warrant optimal adaptation of the tRNA^{Ala} acceptor stem to the specific binding region of the ARS. The increased structural rigidity produced by the insertion of regular Watson-Crick pairs might prevent the constructive interaction between tRNA^{Ala} and ARS by the inability of the tRNA to present functional groups (as, e.g. amino or carbonyl groups), or to adapt the ribose-phosphate backbone, in the required way.

In the recognition of tRNA^{Val} from *E. coli* by its cognate valyl-tRNA synthetase (ValRS), rigidity of the acceptor stem seems to be important [43]. If the anticodons of *E. coli* tRNA^{Ala} and tRNA^{Phe} are replaced by the anticodon of tRNA^{Val}, they become substrates for the ValRS. The efficiency of aminoacylation of both tRNA^{Ala} and tRNA^{Phe} variants with valine is increased if G-U pairs (G3-U70 in tRNA^{Ala}, G4-U69 in tRNA^{Phe}) are replaced by Watson-Crick pairs. Obviously, for optimal interaction between the tRNA and the ValRS a regular A-helical structure in the central part of the acceptor stem is required.

Possibly, for a productive interaction between tRNA^{Ala} and the ARS, the opposite behavior is observed: increased flexibility and/or dynamics in the vicinity of the major identity element, the wobble pair G3-U70, enable a highly efficient adaptation of the acceptor stem to complementary regions of the ARS.

Acknowledgements: We thank Profs. Dr. M. Sprinzl (Bayreuth) and Dr. W.H. McClain (Madison, WI) for helpful discussions and Dr. H. Sklenar (Berlin) for providing the CURVES program. This work was supported by the Deutsche Forschungsgemeinschaft (Projekt Li 722/1-2).

References

[1] Normanly, J. and Abelson, J. (1989) Annu. Rev. Biochem. 58, 1029–1049.
[2] McClain, W.H. (1993) J. Mol. Biol. 234, 257–280.
[3] Hou, Y.-M. and Schimmel, P. (1988) Nature 333, 140–145.
[4] McClain, W.H. and Foss, K. (1988) Science 240, 793–796.
[5] Francklyn, C. and Schimmel, P. (1989) Nature 337, 478–481.
[6] Musier-Forsyth, K., Usman, N., Scaringe, S., Doudna, J., Green, R. and Schimmel, P. (1991) Science 253, 784–786.
[7] Shi, J.-P., Francklyn, C., Hill, K. and Schimmel, P. (1990) Biochemistry 29, 3621–3626.
[8] McClain, W.H., Chen, Y.-M., Foss, K. and Schneider, J. (1988) Science 242, 1681–1684.
[9] Gabriel, K., Schneider, J. and McClain, W.H. (1996) Science 271, 195–197.
[10] McClain, W.H., Gabriel, K. and Schneider, J. (1996) RNA 2, 105–109.
[11] Limmer, St., Reif, B., Ott, G., Arnold, L. and Sprinzl, M. (1996) FEBS Lett. 385, 15–20.
[12] Ramos, A. and Varani, G. (1997) Nucleic Acids Res. 25, 2083–2085.
[13] Ott, G., Arnold, L., Smrt, J., Sobkowski, M., Limmer, St., Hofmann, H.-P. and Sprinzl, M. (1994) Nucleosides Nucleotides 13, 1069–1085.
[14] Puglisi, J.D. and Tinoco Jr, I. (1989) Methods Enzymol. 180, 305–325.
[15] Varani, G. and Tinoco Jr, I. (1991) Q. Rev. Biophys. 24, 479–532.

[16] Legault, P. and Pardi, A. (1994) J. Am. Chem. Soc. 116, 8390–8391.
[17] Legault, A. and Pardi, A. (1997) J. Am. Chem. Soc. 119, 6621–6628.
[18] Brünger, A.T. (1996) XPlor Version 3.851.
[19] Parkinson, G., Vojtechovsky, J., Clowney, L. and Brünger, A.T. (1996) Acta Cryst. D 52, 57–64.
[20] Varani, G., Aboul-ela, F. and Allain, F.H.-T. (1996) Prog. NMR Spectr. 29, 51–127.
[21] Gorenstein, D.G. (1990) Phosphorus-31 NMR: Principles and Applications, Academic Press, New York.
[22] Lavery, R. and Sklenar, H. (1988) J. Biomol. Struct. Dyn. 6, 63–91.
[23] Limmer, St. (1997) Prog. Nucleic Acids Res. Mol. Biol. 57, 1–39.
[24] Hunter, W.N., Anand, N.N. and Kennard, O. (1986) Nature 320, 552–555.
[25] Hunter, W.N., Brown, T. and Kennard, O. (1987) Nucleic Acids Res. 15, 6589–6607.
[26] Wang, C., Gao, H., Gaffney, B.L. and Jones, R.A. (1991) J. Am. Chem. Soc. 113, 5486–5488.
[27] Boulard, Y., Cognet, J.A.H., Gabarro-Arpa, J., LeBret, M., Carbonneaux, C. and Fazakerley, G.U. (1995) J. Mol. Biol. 246, 194–208.
[28] Cai, Z. and Tinoco Jr, I. (1996) Biochemistry 35, 6026–6036.
[29] Saenger, W. (1984) Principles of Nucleic Acids Structure, Springer, New York, p. 108.
[30] Allain, F.H.-T. and Varani, G. (1995) J. Mol. Biol. 250, 333–353.
[31] Pardi, A., Hare, D.R. and Wang, C. (1988) Proc. Natl. Acad. Sci. USA 85, 8785–8789.
[32] Metzler, W.J., Wang, C., Kitchen, D.B., Levy, R.M. and Pardi, A. (1990) J. Mol. Biol. 214, 711–736.
[33] Arnott, S., Hukins, D.W.L. and Dover, S.D. (1972) Biochem. Biophys. Res. Commun. 48, 1392–1399.
[34] Giessner-Prettre, C. and Pullman, B. (1976) Biochem. Biophys. Res. Commun. 70, 578–581.
[35] Arter, D.B. and Schmidt, P.G. (1976) Nucleic Acids Res. 3, 1437–1447.
[36] Giessner-Prettre, C. and Pullman, B. (1987) Q. Rev. Biophys. 20, 113–172.
[37] Hader, P., Alkema, D., Bell, R.A. and Neilson, J. (1982) J. Chem. Soc. Chem. Commun., 10–12.
[38] Beuning, P.J., Yang, F., Schimmel, P. and Musier-Forsyth, K. (1997) Proc. Natl. Acad. Sci. USA 94, 10150–10154.
[39] Limmer, St., Hofmann, H.-P., Ott, G. and Sprinzl, M. (1993) Proc. Natl. Acad. Sci. USA 90, 6199–6202.
[40] Freier, S.M., Kierzek, R., Jaeger, J.A., Sugimoto, N., Caruthers, M.H., Neilson, T. and Turner, D.H. (1986) Proc. Natl. Acad. Sci. USA 83, 9373–9377.
[41] Santa Lucia, J., Kierzek, R. and Turner, D.H. (1991) Biochemistry 30, 8242–8251.
[42] He, L., Kierzek, R., Santa Lucia Jr, J., Walter, A.E. and Turner, D.H. (1991) Biochemistry 30, 11124–11132.
[43] Liu, M., Chu, W.-C., Liu, J.C.-H. and Horowitz, J. (1997) Nucleic Acids Res. 25, 3944–3949.